www.springer.com/41230
https://doi.org/10.1007/s41230-026-5085-6
Special Review CHINA FOUNDRY
Vol. 23 No. 1 January 2026

A review of electroslag remelting composite technologies

Yu Wang[1], *Yan-chun Lou[1], Fang Wang[2], Heng Cao[1], Yun-bao Gao[1], Ling Zhao[1], Zhi Han[1], and Meng Li[3]

1. State Key Laboratory of Advanced Casting Technologies, Shenyang 110021, China

2. School of Metallurgy, Northeastern University, Shenyang 110819, China

3. Liaoning Institute of Science and Technology, Benxi 117004, Liaoning, China

Abstract: Electroslag remelting (ESR) is an important metallurgical process for producing high-purity materials with homogeneous compositions and sound microstructures, and its typical products are ingots or simple castings. The core principle involves the resistive melting of a consumable electrode within a slag pool, followed by the refining of molten metal droplets as they traverse the slag, and subsequent sequential solidification in a water-cooled mold. However, conventional ESR processes face limitations in producing large or complex-shaped components, enhancing production efficiency, achieving highly specialized microstructures, and meeting ultra-high purity demands for advanced applications. Advanced composite ESR technologies have been developed to overcome these limitations by innovatively modifying key process aspects. For instance, electrode systems are improved using vibration, rotation, or multiple electrodes. Enhanced mold design and solidification control are achieved through techniques including conductive molds, mold rotation, and ingot withdrawal. Precise control of the process is realized through the use of protective gas, vacuum, or elevated pressure, as well as the application of external fields such as magnetic fields or ultrasonic vibration. This review comprehensively summarizes these advanced techniques, examining their principles and characteristics, and discussing their specific advantages and challenges.

Keywords: electroslag remelting (ESR); composite electroslag technology; near-net shape casting; high purity materials; process modification; external field assisted casting

CLC numbers: TG146 **Document code:** A **Article ID:** 1672-6421(2026)01-001-19

1 Introduction

High-performance materials are a critical requirement for modern engineering and manufacturing[1]. Additionally, manufacturing demands processes capable of producing large, complex, near-net shape components to minimize machining and material waste[2, 3]. Electroslag remelting (ESR) is identified as a key secondary metallurgy technique[4], offering unique capabilities for refining metals and alloys and producing high-integrity components[5]. The ESR process, whose technical principle is illustrated in Fig. 1[6], progressively melts a consumable electrode through Joule heating generated by an electric current passing through a reactive molten slag. This configuration promotes efficient heat generation, provides atmospheric shielding, facilitates refining reactions, enables effective sequestration of non-metallic inclusions, and ensures controlled heat transfer during solidification in a water-cooled copper mold[7]. As a result, materials produced via ESR demonstrate improved cleanliness, minimized segregation, refined solidification structures, and enhanced mechanical properties compared to those produced by conventional methods. These characteristics make ESR materials highly suitable for applications in aerospace, power generation, tooling, and heavy industries[8]. However, conventional ESR processes have limitations that restrict their use for sophisticated industrial needs. For instance, the production of very large ingots using a single electrode is inherently challenging. Fabricating complex geometries using conventional molds is often impractical; precisely controlling solidification behavior and microstructural evolution remains challenging; and achieving ultra-low levels of gases and impurities is particularly difficult

*Yan-chun Lou
Male, Ph. D., Researcher. He has won two National Prizes for Progress in Science and Technology (both in second place). His research primary focuses on the R&D of foundry materials, casting technology and equipment, and their engineering applications.

E-mail: louych@chinasrif.com

Received: 2025-04-09; Revised: 2025-12-01; Accepted: 2025-12-16

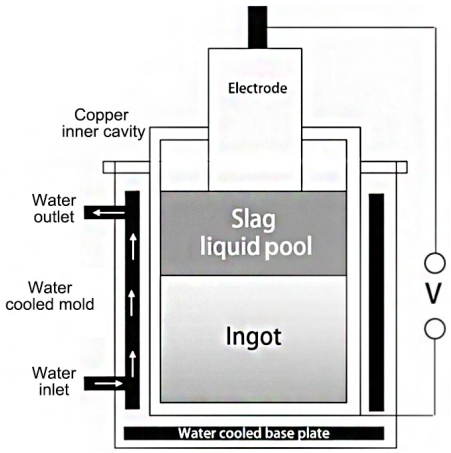

Fig. 1: Schematic diagram of ESR[6]

for certain advanced alloys[9-11].

To overcome the limitations of conventional ESR techniques, substantial research and development have been conducted, and various advanced or "composite" ESR techniques have emerged. Key innovations include: electrode systems that use dynamic actuation or multiple units; mold designs that feature conductive materials or withdrawal systems; process atmospheres with precise control (e.g., pressure, composition); and external physical fields (e.g., magnetic, ultrasonic) that manipulate process dynamics. These composite manufacturing technologies aim to enhance refining and microstructure control, facilitate near-net shape manufacturing, enable the production of functionally graded materials or composite structures, and allow for the processing of novel alloys[12, 13].

This paper reviews the significant progress in advanced ESR technologies. Section 2 discusses electrode system modifications. Section 3 covers mold design and solidification control innovations, including external field assistance. Section 4 details process atmosphere and pressure control techniques. This review integrates recent findings, examines fundamental principles and pertinent challenges, and delineates future research directions within this developing field.

2 Electrode system modifications and innovations

The consumable electrode system, which acts as both the material feedstock and an essential electrical conduit, is a critical focus for technological innovation aimed at expanding operational capabilities and overcoming the inherent limitations of conventional ESR processes. The limitations of the conventional static, single-electrode configuration have been transcended by notable advancements, including the dynamic actuation of electrodes, and the modulation of electrode number and arrangement. This section provides a review of pivotal developments in electrode system modifications, including: (1) the application of mechanical vibrations for melt dynamics and solidification control (Section 2.1); (2) implementation of electrode rotation to harness centrifugal forces for melt flow and refining control (Section 2.2); (3) employment of multi-electrode configurations (twin, triple, or more) for large-scale or hollow ingot production and complex power/heat distribution management (Section 2.3); and (4) advancement of fixed-mobile electrode arrangements and controlled filling methodologies tailored for near-net shape casting of complex geometric components (Section 2.4). These diverse methodologies converge on shared objectives: (1) to achieve superior active control over melt droplet formation, melt pool hydrodynamics, heat distribution, and solidification kinetics compared with conventional ESR; (2) to optimize process efficiency in terms of melting rate and energy consumption; (3) to enhance metallurgical refining efficacy, particularly regarding inclusion removal and microstructural regulation; and (4) ultimately, to extend the manufacturing scope of electroslag technology towards the production of larger ingots, components with complex geometries, or specialized high-integrity material structures. The advancement, understanding, and optimization of these advanced electrode system technologies have relied heavily on sophisticated multiphysics modeling, supported by rigorous experimental validation, thereby providing quantitative insights into complex process dynamics and guiding practical implementation, as elaborated in the ensuing discussion.

2.1 Vibrating electrode technology

By introducing mechanical electrode vibration in ESR process, melt dynamics are actively influenced, resulting in enhanced process control and improved metallurgical quality. The vibrating electrode method, a significant innovation, was proposed and systematically studied by Lou's research team[14]. They systematically advanced the technique through conceptualization, 3D apparatus development, and the creation of comprehensive analytical methods. A significant part of their contribution lies in the development and application of transient, three-dimensional, fully coupled mathematical models to simulate the complex interplay of electromagnetic phenomena, fluid flow (including two-phase flow of metal droplets and slag), heat transfer, and solidification behavior within the vibrating electrode ESR system[15]. These advanced computational models, often solved using finite element or finite volume methods, and incorporating techniques like the volume of fluid (VOF) method for tracking droplet formation and the enthalpy method for solidification, allowed for detailed prediction of electric fields, velocity fields, temperature distributions, Joule heating patterns, and droplet sizes/distribution under various vibration conditions (including horizontal and vertical vibrations with different amplitudes and frequencies). Crucially, these modeling efforts were closely coupled with experimental verification (Fig. 2[16]), comparing the vibrating electrode process against conventional ESR and validating the simulation results[16-17].

The research demonstrated that electrode vibration fundamentally altered the droplet detachment process, shifting it from a random, scattered behavior in traditional ESR to a more ordered and periodic detachment under vibration (Fig. 3)[14]. This altered dynamic, combined with induced stirring effects, was

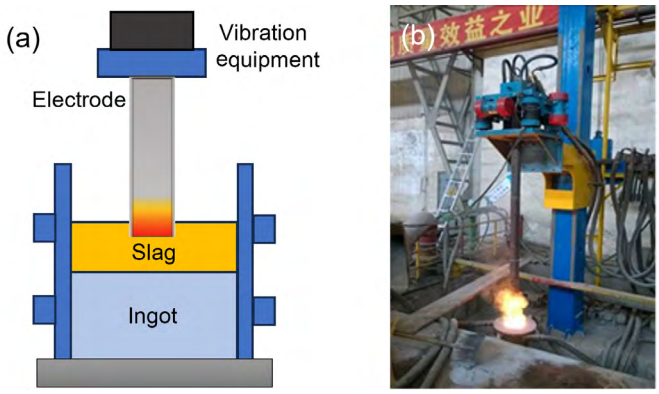

Fig. 2: Vibrating electrode assisted ESR model (a) and ESR experiment with the vibrating electrode (b)[16]

shown to significantly enhance process efficiency; specifically, the vibrating electrode method could increase the electrode melting rate by over 20% compared to conventional ESR, with corresponding energy savings reported to be maximized up to 17% at an optimal vibration frequency of approximately 20 Hz (Fig. 4)[16, 17]. Comparative studies within their work also indicated that vertical electrode vibration generally exerts a more pronounced effect on increasing the melt rate than vertical vibration (a finding consistent between numerical simulations and experimental measurements), potentially linked to differences in the induced heat transfer coefficients between the two vibration modes[15, 17]. Beyond efficiency gains, significant metallurgical benefits were observed. Electrode vibration was found to refine the grain structure within the solidified ingot, particularly in the central region, and contribute to the reduction or elimination of undesirable Widmanstatten structures[16]. Furthermore, appropriate electrode vibration parameters proved effective in improving the cleanliness of

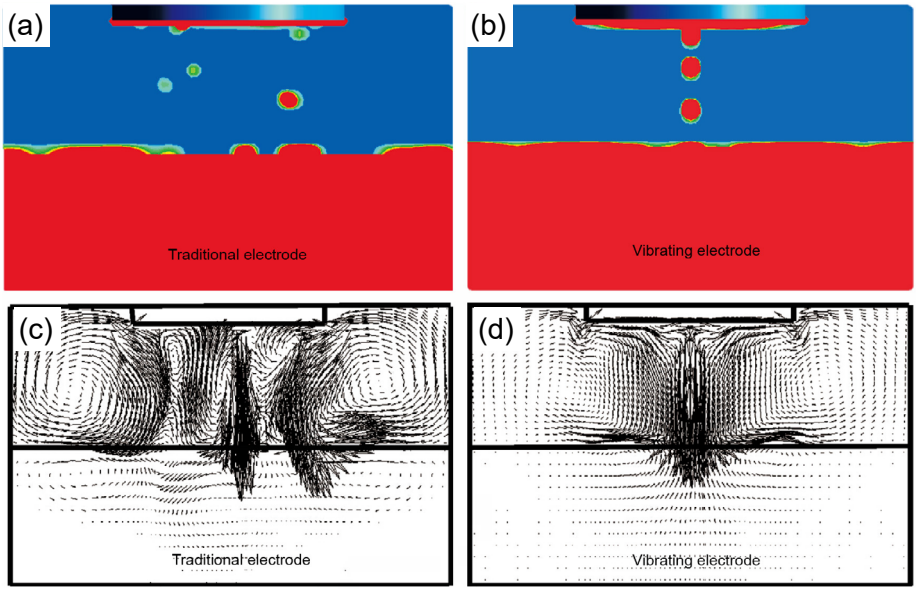

Fig. 3: Drop process of metal droplets (a, b) and velocity field (c, d) of the vertical section in ESR process with traditional electrode (a, c) and vibrating electrode (b, d)[14]

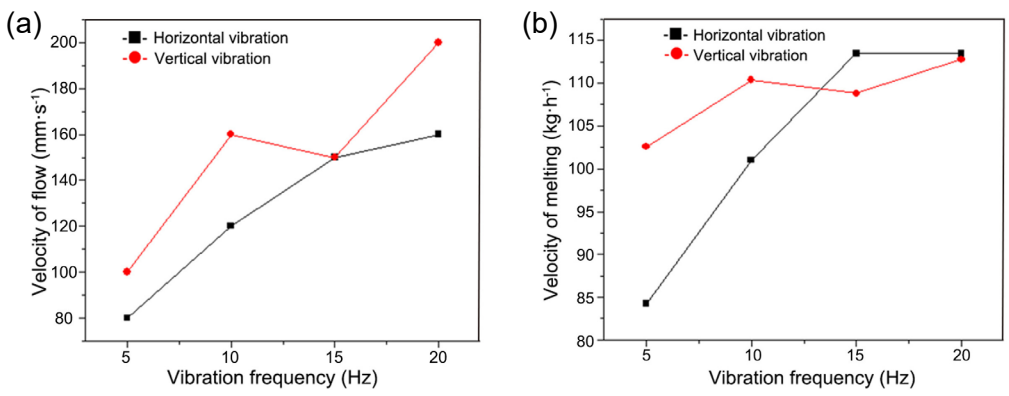

Fig. 4: Dependence of velocity of flow (a) and melting (b) on vibration frequency[16]

the steel by reducing the overall quantity and average size of non-metallic inclusions, particularly mitigating large-sized inclusions[18].

Consequently, the above research validated vibrating electrode technology as an advanced ESR technique, yielding quantifiable improvements in melting efficiency, energy consumption, solidification structure and inclusion control, and providing optimized parameters for practical applications. However, the optimization of vibration frequency and amplitude is complex, requiring extensive experimental validation. The mechanisms by which different vibration directions affect melting rate and solidification structure still require further in-depth research.

2.2 Rotating electrode technology

The rotational actuation of the consumable electrode around its longitudinal axis during ESR constitutes a dynamic modification, which is designed to actively modulate melting phenomena, molten pool hydrodynamics, heat transfer, and solidification behavior[19]. The fundamental mechanism is the action of centrifugal forces on the molten metal film at the electrode tip[20], as shown in Fig. 5[21]. The equilibrium liquid flow at the melting electrode tip is governed by the synergistic interaction of centrifugal, gravitational, surface tension, and electromagnetic forces, and the corresponding remelting parameters have been optimized thorough analytical computations[22]. Transient three-dimensional (3D) coupled multiphysics simulations, incorporating magnetohydrodynamics (MHD), VOF interface tracking, large eddy simulation (LES) turbulence modeling, and adaptive mesh refinement, have been extensively employed to analyze these synergistic effects and optimize the process parameters[23].

Numerical simulations consistently indicate that electrode rotation induces marked alterations in melting dynamics. These changes include a flattened electrode tip profile, a significant reduction in horizontal deviation (e.g., 69.9%[23]), a decrease in liquid metal film thickness with increasing rotation speed[23], and a transition in metal droplet detachment from central to peripheral regions[21], accompanied by a decrease in the detached droplet equivalent diameter[23]. Compared to buoyancy-driven flow in conventional ESR, electrode rotation induces forced convection, resulting in distinct modifications to the fluid flow and temperature distribution within the slag and metal pools[23, 24]. An upward heat flux in the slag bath, attributed to electrode rotation, is suggested to improve mold heat utilization[20]. These hydrodynamic and thermal changes directly impact the solidification process, leading to a shallower and flatter metal pool profile as rotation speed increases[23, 25] (Fig. 6[25]).

From a metallurgical quality perspective, electrode rotation is posited to modulate ingot solidification microstructure, encompassing grain orientation and crystallographic texture, thereby affecting anisotropic properties[19, 20]. Furthermore, a significant benefit highlighted in recent modeling work is the enhanced removal efficiency of non-metallic inclusions,

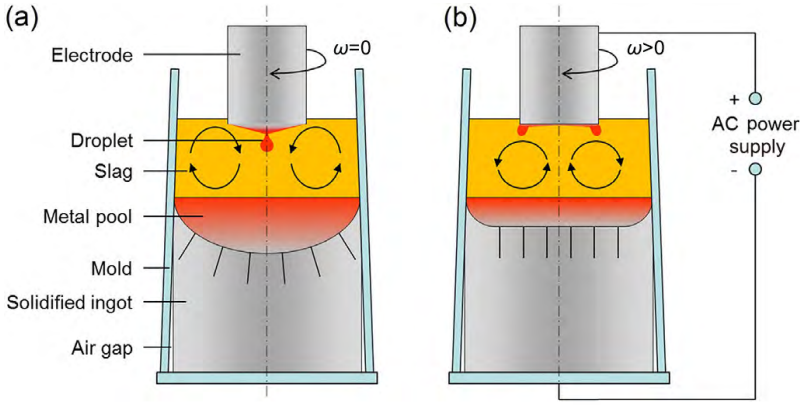

Fig. 5: Schematic of ESR processes with a static electrode (a) and a rotating electrode (b)[21]

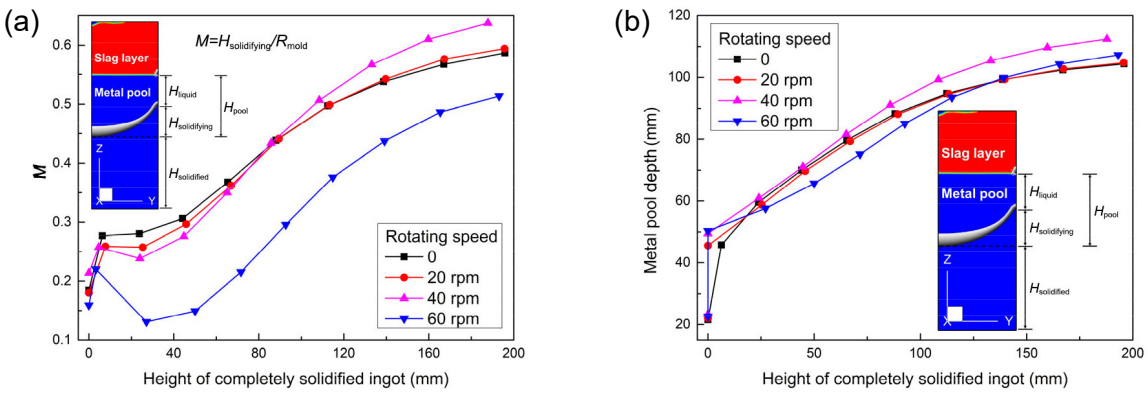

Fig. 6: Evolution of metal pool profile with the electrode rotating at different speeds: (a) *M* (ratio of the height of metal being solidified to the radius of the mold); (b) metal pool depth[25]

i.e., electrode rotation dramatically increases the specific surface area available for slag-metal interaction and modifies inclusion trajectories, and thereby improves metal cleanliness[21, 24], as shown in Fig. 7[21]. Beyond structural and cleanliness improvements, the application of rotating electrode ESR technology has also demonstrated tangible benefits for material properties, such as enhancing the corrosion resistance of low-carbon chromium-containing steels relative to their conventionally processed counterparts[26].

Collectively, these investigations demonstrate electrode rotation as a robust technique for advanced ESR, facilitating the control of melt dynamics, optimization of heat transfer, tailoring of solidification parameters, enhancement of metal purity, and potential improvement of remelted material properties. Engineering challenges associated with the rotating device, particularly sealing integrity, reliable electrical conductivity, and cooling water problems, require urgent resolution, especially for large-scale industrial applications. Furthermore, finding the optimal rotation speed to balance melting efficiency and solidification structure is a bottleneck.

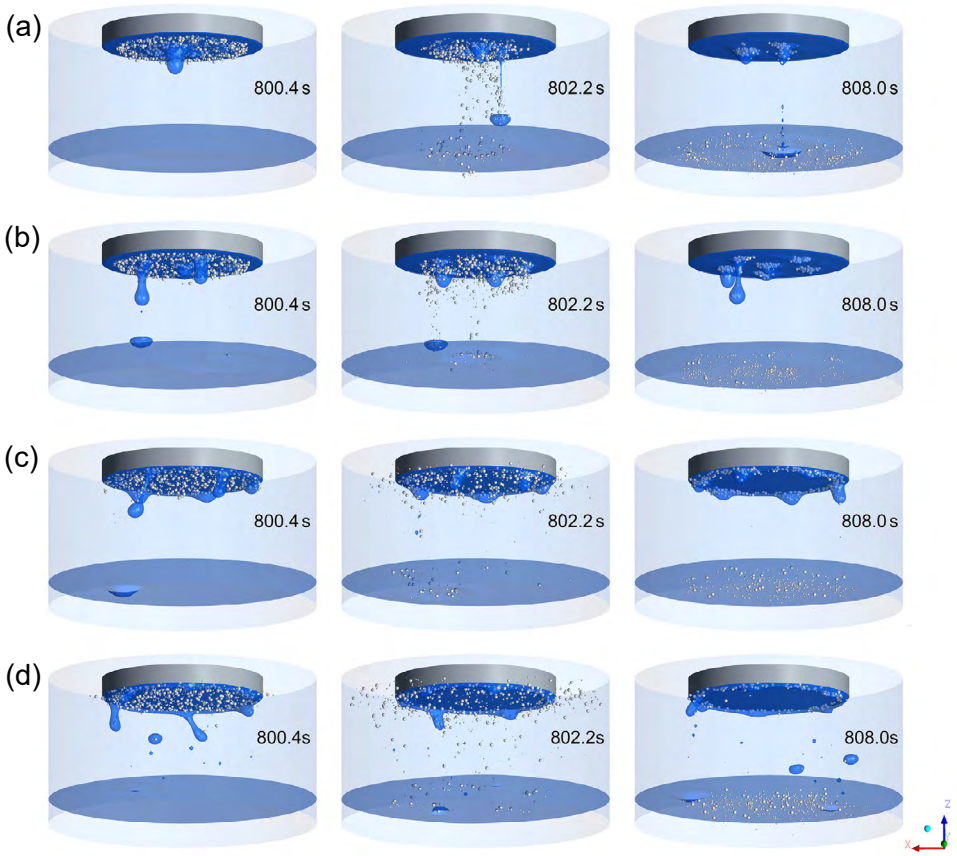

Fig. 7: Transient formation and dripping process of metal droplets at different electrode rotation speeds: (a) 0 rpm; (b) 20 rpm; (c) 40 rpm; (d) 60 rpm. The deformation of the slag/metal interface is presented by 0.5 local volume fraction of metal[21]

2.3 Multiple electrode technology

Multiple electrode ESR technology represents a significant process adaptation primarily developed to overcome the scalability and efficiency limitations inherent in single-electrode systems. This innovation enables the production of large-dimension ingots (such as heavy forging ingots[27-31] and thick slabs[32, 33]) and complex geometries required for specialized applications (e.g., large hollow ingots[34, 35]). Diverse configurations have been implemented and studied, including twin-electrode systems (often operated in series or bifilar mode)[28, 32, 33], triple-electrode arrangements[29-31], and even six-electrode three-phase furnaces (for ultra-heavy ingot production) using bifilar or monofilar power supply schemes[27]. These multi-electrode configurations are often integrated with other advanced ESR variations, such as T-shaped mold ingot withdrawal for large slab ingots (3.2 m×1.4 m×4.0 m, offshore jack-up platform rack steel[29, 32]) or electroslag remelting with up-pulling inner mold (EUPIM) method for large hollow cylindrical castings (Fig. 8)[34, 35].

To understand the underlying physics and optimize process parameters in multi-electrode ESR, comprehensive mathematical modeling is indispensable due to the process' complexity and scale. To simulate multi-electrode ESR systems, numerous studies have utilized transient, three-dimensional, coupled multiphysics models. These models integrate the finite element method (FEM) for electromagnetic fields analysis, computational fluid dynamics (CFD) for fluid dynamics (often incorporating turbulence models like k-ε), heat transfer, and enthalpy-based solidification models[28-31, 34]. Research has revealed distinct electromagnetic behaviors in multi-electrode configurations. For instance, modeling of twin series-connected systems indicates that the majority of the electric current flows

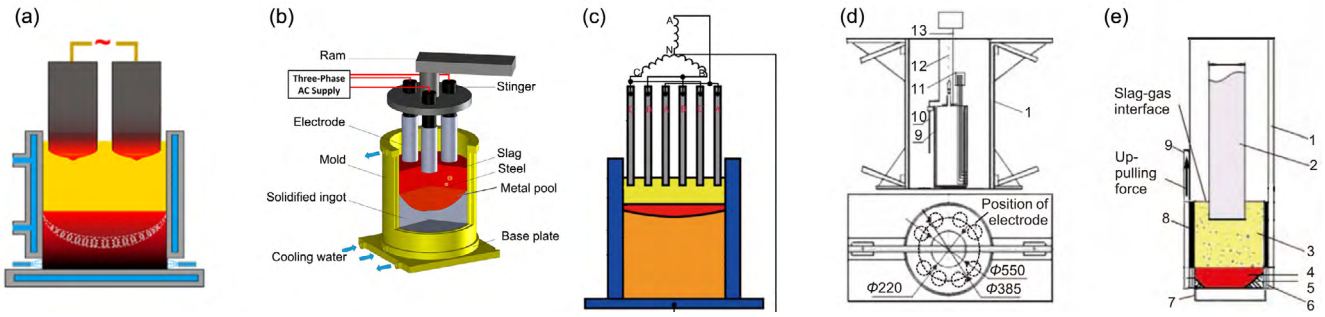

1. Outer mold; 2. Consumable electrode; 3. Slag pool; 4. Metal basin; 5. Solidified casting; 6. Gas gap;
7. Bottom water tank; 8. Slag shell; 9. Inner mold; 10. Sensor; 11. Residual stress test instrument;
12. Up-pulling linkage control equipment; 13. Guide bar

Fig. 8: Electroslag remelting withdrawing (ESRW) process with bifilar mode and T-shaped mold[32] (a); schematic of the ESR process with triple-electrode[31] (b); diagrams of three-phase bifilar of ESR[27] (c); ESR up-pulling inner mold method equipment[35] (d); schematic of the initial up-pulling process[35] (e)

through the slag layer, particularly near the slag/ingot interface. Furthermore, a noticeable 'neighbor effect' between the closely spaced electrodes significantly suppresses the electromagnetic skin effect compared to single-electrode operation[28]. The magnetic flux density exhibits specific patterns, being reinforced in the region between the electrodes and reduced outside them[28]. In three-phase six-electrode systems, the geometrical arrangement of electrodes (e.g., close proximity of bifilar pairs versus equidistant spacing) and the type of electrical connection (bifilar vs. monofilar) critically influence the uniformity of potential and heat generation distribution, with monofilar connections generally providing the most uniform distribution and potentially more favorable magnetic field conditions (as shown in Fig. 9)[27].

Joule heating, the primary heat source, is typically concentrated near the electrode tips and the slag/electrode interface, and its distribution is sensitive to parameters such as electrode immersion depth[28, 30]. These characteristics govern the resulting fluid flow patterns (the flow patterns can be intricate, often featuring multiple interacting vortices, as shown in simulations of triple-electrode systems[31]), and ultimately control the heat distribution across the large slag and metal pools. This capacity to regulate the thermal profile is crucial for controlling the shape and depth of molten metal pool, as well as ensuring desirable solidification conditions across the large cross-section of the ingot or casting[33-35], as can be found from Fig. 10[30].

Therefore, multi-electrode ESR technology, supported by advanced modeling, provides essential means for scaling up the electroslag process to produce large-tonnage, high-quality ingots and complex castings demanded by modern industries. However, the complex equipment structure and control system increase costs and operational difficulty. The main challenges involve achieving synchronized control of multiple electrode melting rates, preventing inter-electrode short circuits, and ensuring uniform structure throughout the cross-section of large ingots.

2.4 Fixed-movable electrode and controlled filling technologies

Due to the constraints of mold cavities, conventional ESR is limited in producing components with complex geometries. Consequently, controlled filling strategies, such as the filling method of fixed consumable electrode (FMFCE), have been developed for manufacturing components with non-conventional mold cavities[36-38]. FMFCE technique, which employs parallel fixed-movable dual electrodes, enables the fabrication of complex castings through the controlled fusion of electrode materials to progressively fill intricate molds or construct specific features[36], as shown in Fig. 11[38].

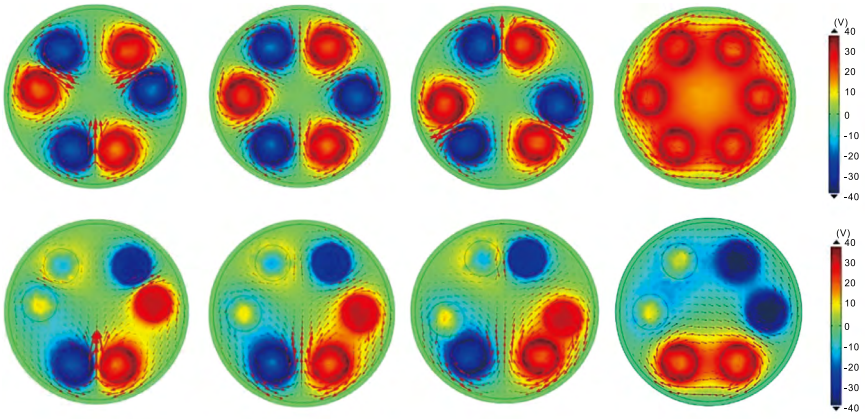

Fig. 9: Distribution of electric potential (given by colors) and magnetic flux density (indicated by arrows) for simulated configurations of consumable electrode locations and electrical connections[27]

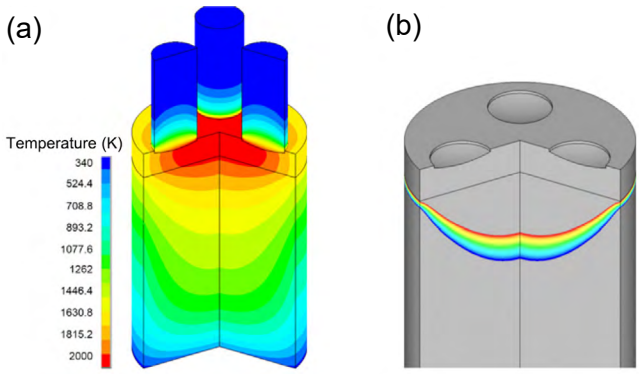

Fig. 10: Distribution of temperature (a) and metal pool profile (b) in an electroslage remelted ingot at 6,000 s with a triple-electrode configuration[30]

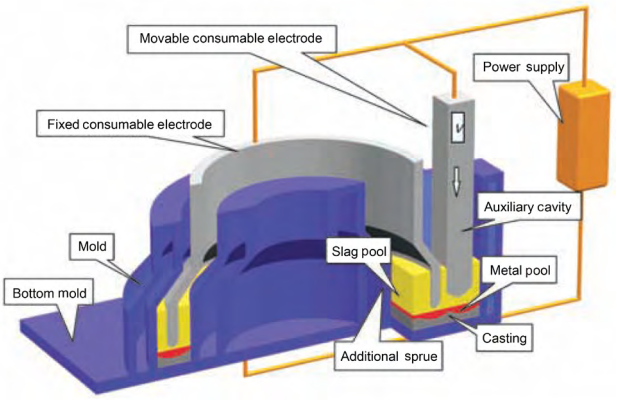

Fig. 11: Schematic of the parallel fixed-movable dual-electrode ESR setup[38]

Achieving a stable and predictable casting process requires a quantitative understanding of the dynamic interactions between the participating electrodes (fixed and movable), and research has extensively characterized these dynamics, especially during stable melting periods. To delineate the optimal correlation for stable filling in parallel fixed-movable dual electrode configurations, a mathematical model $y=kx^2+(k+1)x$, relating current ratio y to electrode cross-sectional area ratio x via a filling ratio k, has been established, and experimental validation indicated specific ratio ranges (e.g., current ratio>1.536, area ratio>0.5) conducive to obtaining high-quality castings[39]. Subsequent investigations on FMFCE dynamics demonstrated that, during stable operation, the average melting rate ratio of electrodes aligns closely with their current ratio[40]. Furthermore, empirical studies established direct proportionality between the average melting rate ratio and the electrode cross-sectional area ratio (proportionality constant ≈ 1.44)[38], as well as between the average melting rate ratio and the electrode equivalent diameter ratio (proportionality constant ≈ 2.09)[40] (Fig. 12[38]).

In addition to stable operational regimes, the nascent stage (particularly the formation of the ingot bottom) plays a crucial role in ensuring the overall integrity of complex castings. Experimental casting trials and numerical simulations have been combined to investigate the bottom formability of plate-shaped ingots (e.g., 400 mm×60 mm cross-section) fabricated via the FMFCE (Fig. 13)[41]. Through these investigations, the stability and controllability of the melting process were substantiated, and the

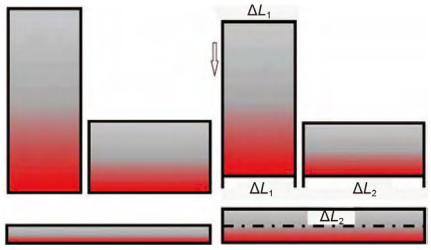

Fig. 12: Process model of parallel fixed-movable dual electrodes ESR[38] (ΔL_1 represents the movable consumable electrode length, and ΔL_2 represents the fixed consumable electrode length)

substantial impact of initial process parameters (particularly the starting current magnitude) on the resultant morphology (concavity or convexity) of the ingot bottom was elucidated. These results provide clear guidelines for optimizing start-up procedures to ensure the sound formation of the ingot bottom.

Consequently, the FMFCE and related controlled filling methodologies, underpinned by quantitative process dynamic analysis and simulation-based optimization, constitute a pivotal advancement in ESR, extending its capacity for the near-net shape fabrication of complex, high-integrity components. However, the process control is complex, especially the precise control of initial parameters. The complexity of the equipment structure and operational procedures also limits its application in the production of extra-large castings.

3 Mold and solidification control technologies

In addition to innovations targeting the electrode system, substantial advancements in ESR technologies have centered on the active control of solidification, which critically determines the ultimate microstructure, compositional homogeneity, and metallurgical integrity of ingots or castings. This control is realized through strategic modifications to the mold system, including material properties, electrical dynamics, and operational kinematics, as well as the external physical fields applied during solidification. This section provides an in-depth exploration of several pivotal strategies developed for advanced mold and solidification control. Strategies include: (1) using conductive/current-carrying molds for modifying thermal/electrical boundaries, as well as ingot withdrawal for enabling semi-continuous operation and regulating solidification (Section 3.1); (2) refinements by applying mold rotation or ultrasonic vibrations to influence solidification, thereby enhancing microstructural homogeneity, inclusion cleanliness, and material density (Section 3.2); and (3) using external magnetic fields to electromagnetically control molten metal flow/heat via Lorentz forces for non-contact solidification, microstructure, and inclusion control (Section 3.3). Collectively, these diverse technologies strive to transcend the predominantly passive solidification control inherent in conventional static molds, offering active methodologies to manipulate temperature gradients, melt convection, solidification front morphology,

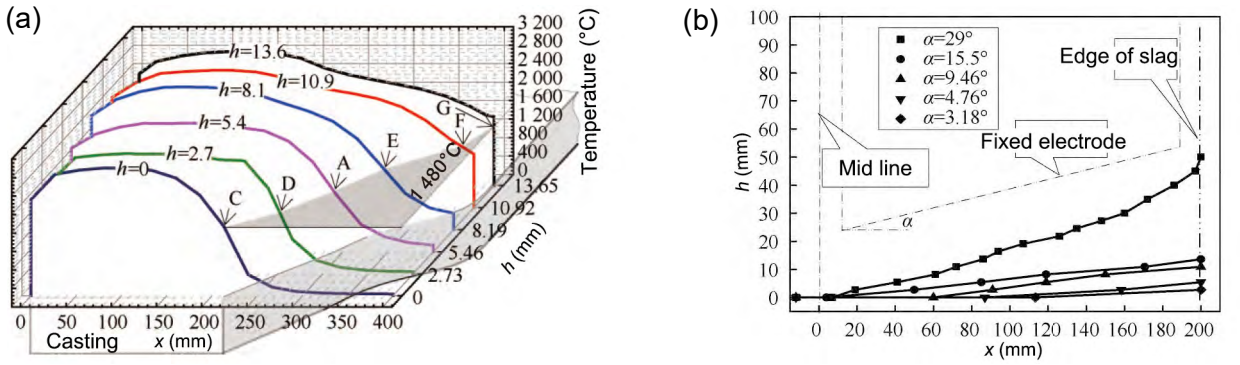

Fig. 13: Calculation results of bottom shape of ingot (a) and effect of bottom angle of fixed electrode on bottom shape of ingot (b)[41] (*h* is the melting height of the ingot, *x* is the lateral distance of the ingot, *α* is the angle at the bottom of the fixed electrode)

phase formation (e.g., carbides), and the behavior of non-metallic inclusions. Objectives include achieving refined microstructures, improved cleanliness and density, near-net shape casting (via conductive molds), and large-scale production, thereby expanding the applications of electroslag materials.

3.1 Advanced mold and solidification control: Conductive molds and ingot withdrawal

By integrating conductive molds and ingot withdrawal, ESR technology achieves precise control over heat transfer, solidification patterns, process kinematics, and final component dimensions, thereby enabling industrial-scale semi-continuous and continuous production. The development of electroslag remelting with current conductive stationary molds (ESR-CCSM)[42] and related methodologies, such as single power dual-circuits electroslag remelting with a current-carrying mold (ESR-STCCM, as shown in Fig. 14)[43], represents a significant difference from traditional water-cooled copper mold practices. These configurations integrate the mold into the electrical circuit, resulting in radically altered current pathways and Joule heating distributions compared to conventional ESR[44].

The current distribution ratio between the electrode and conductive mold, as revealed by numerical simulations and physical modeling using wood's alloy and NaCl solution, is sensitive to filling ratio and electrode immersion depth, but is less sensitive to conductor height[43]. This alters electromagnetic field, in turn, influences the thermal field and fluid flow. Specifically, ESR-STCCM has been demonstrated to produce a shallower molten steel pool and a narrower mushy zone compared to conventional ESR, which potentially confers advantages in mitigating segregation[44]. Moreover, specific power configurations, such as the 'up power' mode in ESR-STCCM, can induce elevated temperatures at the slag-metal interface (Fig. 15), thereby contributing to enhanced ingot surface smoothness[44]. Although current-conductive mold ESR features an altered heat generation pattern (characterized by maximum Joule heat density near the electrode corner and slag/mold interface), its inclusion removal capability is not diminished compared to conventional ESR[45]. Simultaneously, the implementation of process kinematic modifications facilitated by ingot withdrawal technology, alternatively termed drawing-ingot-type ESR[46] and evolving toward continuous casting electroslag rapid remelting (CC-ESRR)[47], serves to mitigate the batch-processing limitations inherent to traditional ESR. This technique entails the progressive withdrawal of the solidified ingot from the base of a truncated, open-ended, or geometrically tailored mold (e.g., T-shaped for slabs), enabling the fabrication of ingots or billets with longitudinal dimensions significantly exceeding the mold's physical height[32, 48]. Electroslag remelting withdrawal (ESRW) plays a pivotal role in the production of large-scale products, including thick slab ingots (e.g., 3.2 m×1.4 m×4.0 m) for applications such as offshore platform rack steel[32, 33], and elongated billets suitable for direct rolling, thus potentially eliminating intermediate forging processes[47].

Mathematical modeling, particularly three-dimensional simulations, plays a crucial role in elucidating the intricate multiphysics phenomena in ESRW. It enables the determination of flow fields, temperature distributions, and molten pool configurations across a spectrum of operating

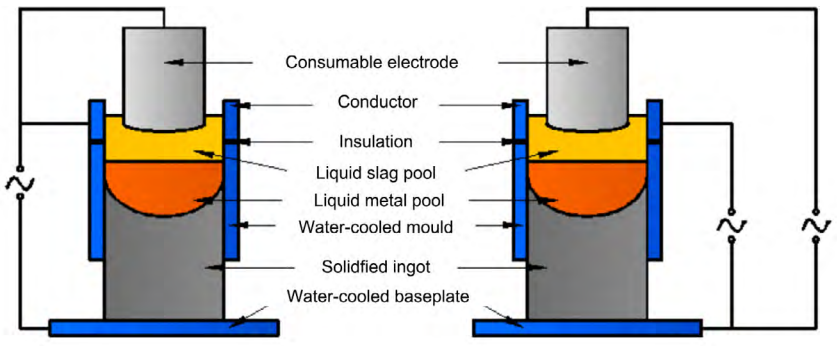

Fig. 14: Schematic diagram of single power or double power dual-circuit ESR[43]

conditions, including electrode immersion depths and slag heights[33, 49, 50]. ESRW also provides a platform for controlling the chemical composition throughout the extended remelting process, as demonstrated by studies on the behavior of alloying element in stainless steels[46]. Note that the implementation of ESRW necessitates specialized equipment, including electrode exchange systems, Ar protection devices, withdrawal mechanisms, and sub-mold secondary cooling systems[48]. Nevertheless, effective operational control, particularly the management of slag composition to ensure stable ingot withdrawal and prevent defects such as steel leakage, requires precise regulation of parameters like melting rate and cooling intensity[51].

In summary, the application of conductive/current-carrying molds and the implementation of ingot withdrawal methodologies constitute advanced modifications to both the solidification environment and process kinematics in ESR. These modifications significantly expand the versatility of ESR technology, enabling enhanced quality control, near-net shaping, and large-scale industrial production. The difficulty in precisely controlling the withdrawal speed to maintain a stable molten pool depth and prevent ingot leakage is a key engineering challenge. Meanwhile, equipment investment and operating costs are high as additional withdrawal mechanisms and secondary cooling systems are required.

3.2 Solidification enhancement via mold rotation and ultrasonic vibration

To improve ingot quality in ESR, researchers have investigated techniques that apply external motion or energy fields to directly modulate the solidification environment within the mold, supplementing modifications targeting the primary melting and refining phases. These approaches enhance microstructural homogeneity and cleanliness, addressing issues exacerbated in large ingots due to reduced conventional mold cooling efficiency[52].

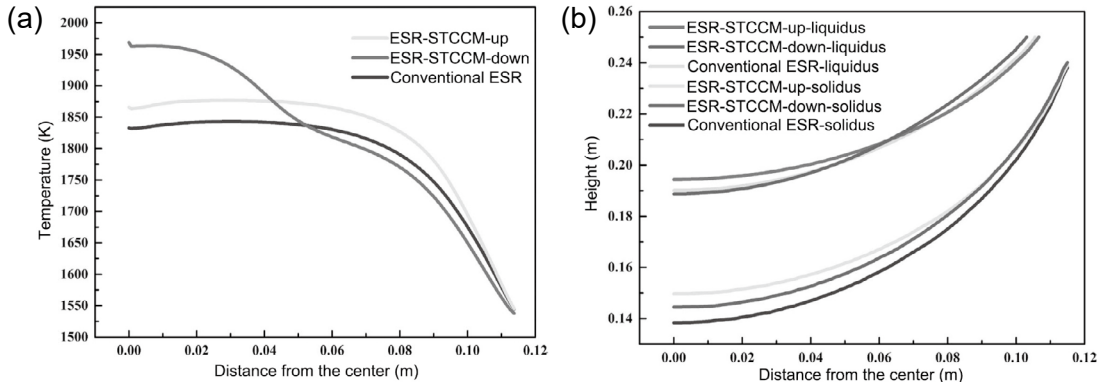

Fig. 15: Temperature distribution of slag/metal interface (a), liquidus and solidus line position for different ESR processes (b)[44]

A specific technique employed involves the rotational actuation of the mold assembly during the ESR process (Fig. 16[53]). Bifilar ESR experiments show that mold rotation (up to 28 r·min^{-1}) improves the chemical uniformity (e.g., C and Cr) and density of ingot[52, 53]. Notably, this homogenization extends to microstructural refinement. For M2 high-speed steel, mold rotation refines and homogenizes the distribution of carbides (e.g., MC, M_6C, and M_2C) while reducing their average dimensions[54]. Moreover, mold rotation significantly impacts non-metallic inclusions, notably reducing their number density and area fraction, especially for those exceeding 5 μm in size. It may also modulate the relative proportions of various inclusion types, such as decreasing Al_2O_3 while increasing complex oxides or sulfides[55]. Empirical investigations have also documented a reduction in the mean dimensional characteristics of Al_2O_3 inclusions, with their size decreasing from 4.4 μm to 1.9 μm, as a function of rotational velocity increasing up to 28 r·min^{-1}[53]. The proposed mechanisms underlying these benefits involve the induced motion promoting a more uniform temperature distribution within the slag and metal pools, enabling more even dispersion of metal droplets, and consequently leading to a flatter solidification front, as supported by numerical simulations[53, 54]. Additionally, mold rotation has been observed to increase the remelting speed, which may potentially reduce power consumption[53]. However, optimizing the rotational speed is crucial, as excessively high speeds can paradoxically deteriorate the solidification structure and impair inclusion removal efficiency[52, 53, 55].

An alternative approach to modulate solidification during ESR involves the introduction of ultrasonic vibrations, as schematically depicted in Fig. 17(a)[56]. The fundamental principles involve acoustic cavitation and streaming, which can induce mixing, degassing, and affect nucleation and growth during solidification[57]. Experimental investigations of ultrasonic power application through the mold wall during ESR have shown positive effects on ingot quality within specific parameter ranges. In particular, improved uniformity in the elemental distribution of Si, Mn, and Cr was observed at ultrasonic power inputs between 300–750 W, with carbon distribution revealing a more complex response, as shown in Fig. 17(b)[56]. Similar to mold rotation, the effectiveness of ultrasonic treatment is highly dependent on the applied power, with excessive power levels potentially failing to improve and even degrading the uniformity and compactness (Fig. 18)[56, 57]. Consequently, both mold rotation and ultrasonic vibration

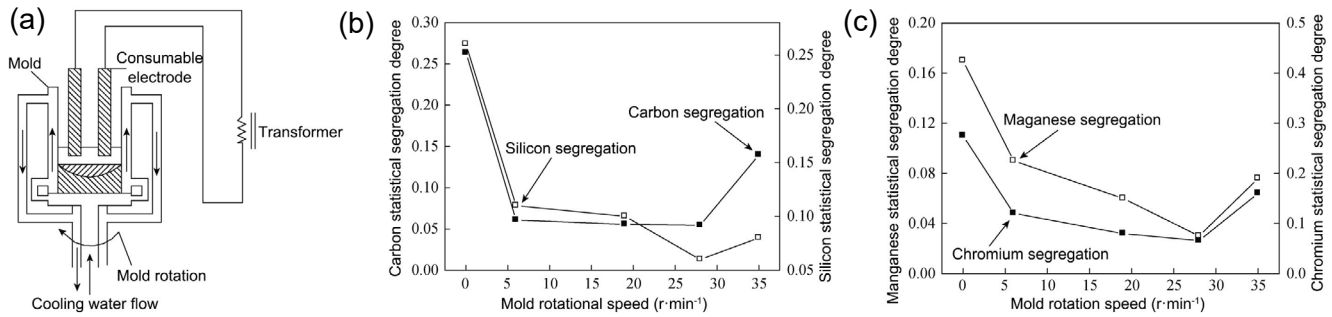

Fig. 16: Schematic of Bifilar ESR furnace with mold rotation (a), and effect of mold rotational speed on the statistical segregation of C and Si (b), and Mn and Cr (c)[53]

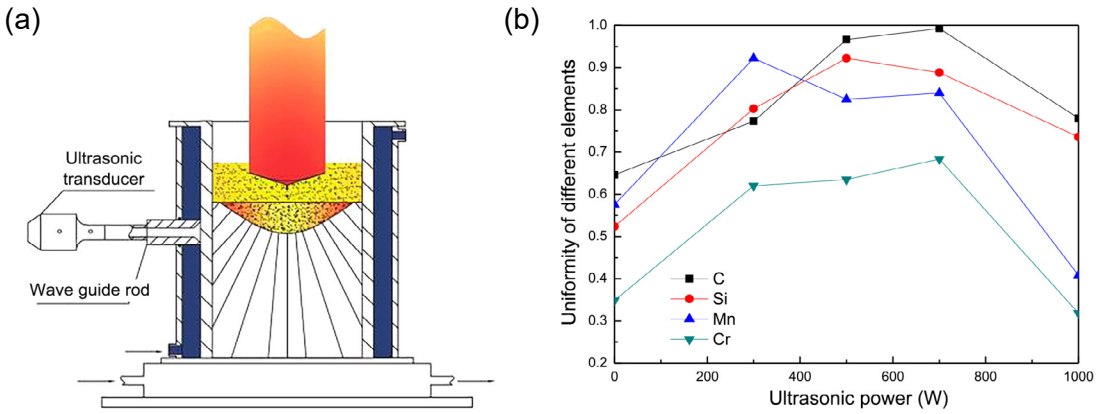

Fig. 17: Schematic diagram of ESR with ultrasonic vibration (a) and effect of ultrasonic power on distribution of alloying elements in steel (b)[56]

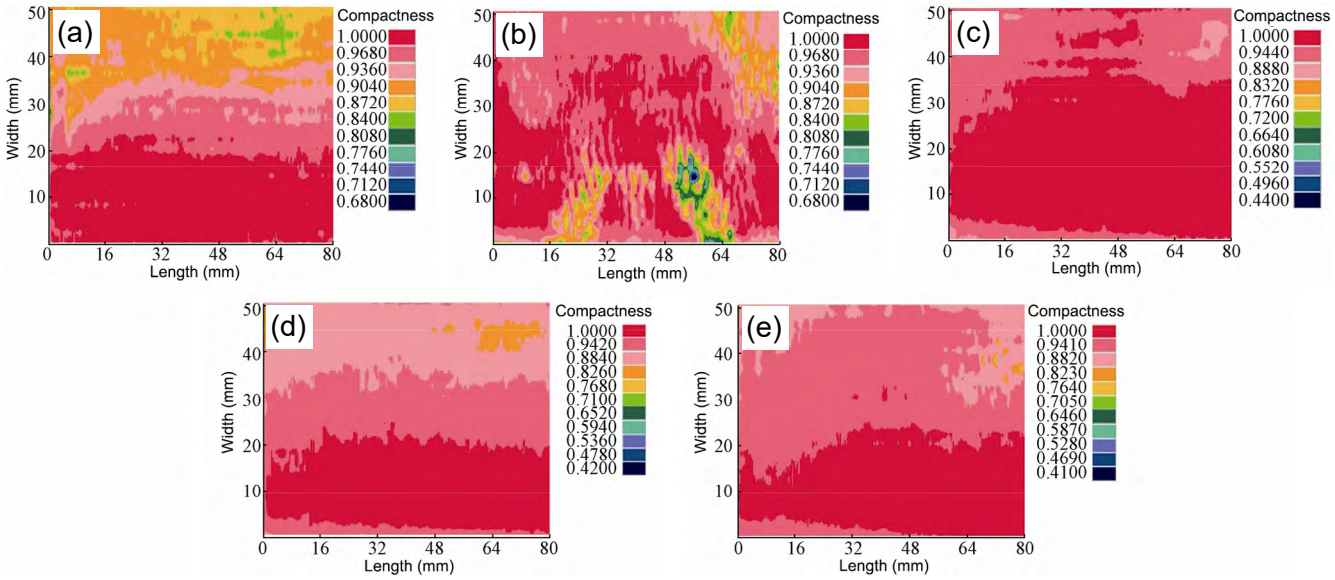

Fig. 18: Effects of ultrasonic power on the compactness of electroslag ingots: (a) 0 W; (b) 300 W; (c) 500 W; (d) 700 W; (e) 1,000 W[57]

assistance emerge as viable yet parameter-sensitive strategies in the advanced ESR toolkit. They enable active manipulation of the solidification process, ultimately achieving enhanced structural homogeneity, improved cleanliness, and increased density in the final product. A core challenge of these technologies lies in their high sensitive to process parameters. For example, excessive ultrasonic power can lead to the deterioration of the solidified structure. Another key bottleneck lies in scaling them up from laboratory research to large-scale, stable industrial production.

3.3 Solidification control via magnetic field assisted technology (MC-ESR)

The application of external magnetic fields during ESR [MC-ESR, with the schematic diagram shown in Fig. 19(a)] constitutes a sophisticated strategy for process modulation,

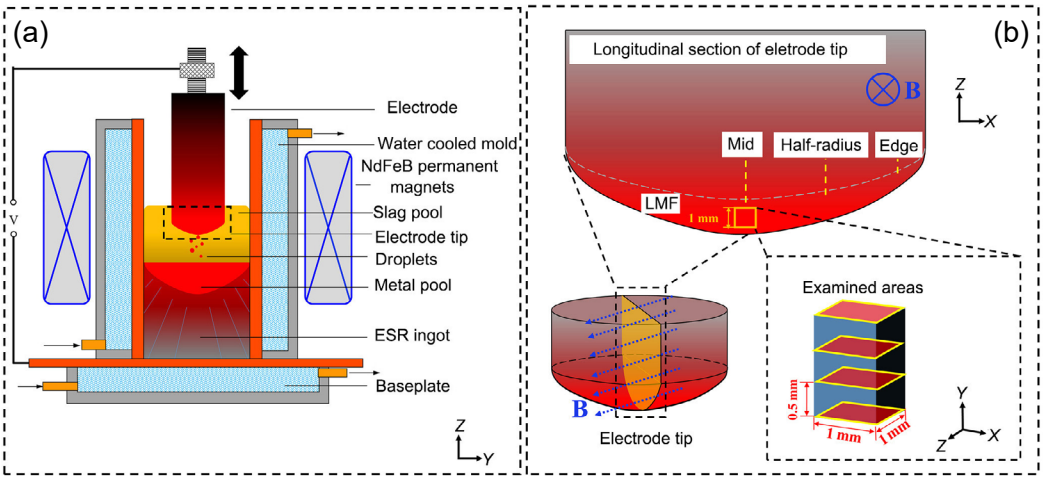

Fig. 19: Schematic diagram of MC-ESR apparatus (a) and sampling method for inclusion detection in LMF (b)[60]

primarily leveraging the Lorentz forces generated by the interaction between the magnetic field and electric current in the conductive slag and metal phases. Beyond fundamentally influencing fluid flow and electrodynamics, these forces provide a potent non-contact approach to actively manipulate heat transfer characteristics and molten pool behavior, thereby enabling precise control over the solidification process and the resultant ingot quality[58, 59].

Different types of magnetic fields have been investigated, including transversal static magnetic fields (TSMF)[60-62], axial static magnetic fields (ASMF)[63], general electromagnetic stirring (EMS) configurations[59], and considerations for direct current (DC) operation[64]. These applied fields demonstrably alter the phenomena occurring at the electrode tip and within the molten pools, directly influencing solidification precursors. For instance, TSMF has been shown via visualization experiments to significantly affect droplet evolution, causing the liquid metal neck to break up into numerous smaller droplets, particularly when low-frequency AC currents (e.g., <100 Hz) are employed. This effect is attributed to the Lorentz forces overcoming surface tension, as shown in Fig. 20[61, 62]. TSMF also accelerates the dynamic processes of the liquid melt film (LMF) at the electrode tip, leading to a reduction in its average thickness (e.g., by up to 41.3% at 95 mT)[60]. Similarly, ASMF induces a spin-vibration effect at the electrode tip, also resulting in a thinner liquid melt film and smaller detached droplets (Fig. 21)[63]. These modifications to melting dynamics and the induced alterations in fluid flow contribute to changes in the solidification conditions. Both TSMF and ASMF applications have been reported to yield a shallower and flatter molten metal pool profile compared with conventional ESR[58, 63], thereby facilitating more uniform solidification and

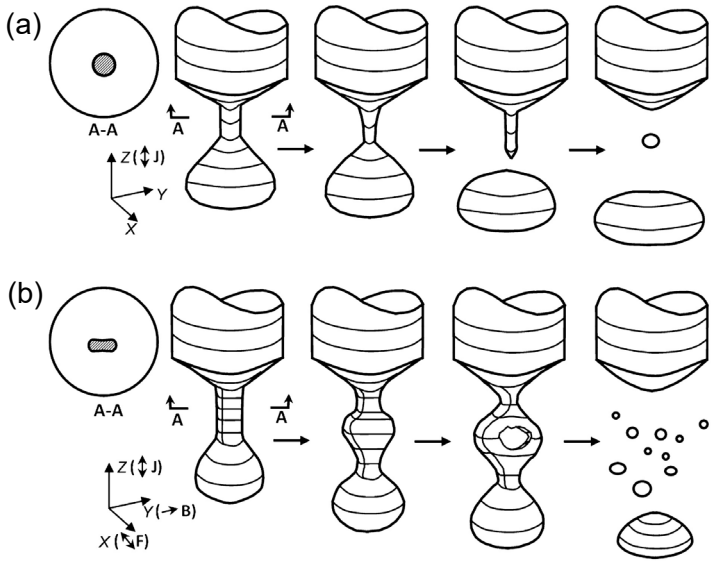

Fig. 20: Schematic three-dimension diagrams of droplet detachment in ESR: (a) without external magnetic field; (b) with the TSMF ≥ 0.5 T[62]

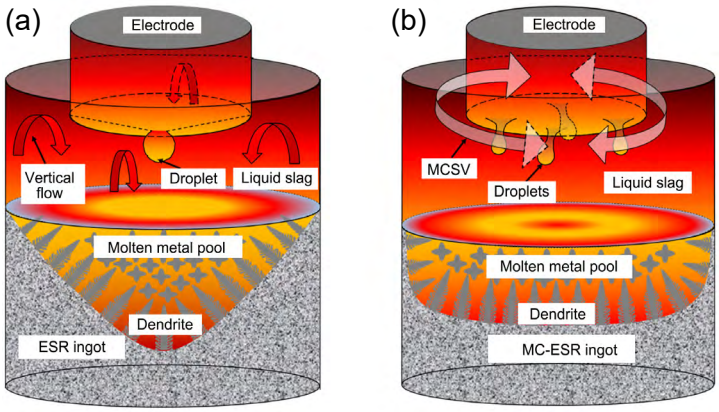

Fig. 21: Schematic diagrams illustrating the effects of ASMF during solidification process: (a) ESR process without magnetic field; (b) MC-ESR process in the presence of ASMF[63]

reducing defects. Consequently, significant improvements in the solidified microstructure have been observed: TSMF application during ESR of M2 high-speed steel led to refined eutectic carbides (MC and M_6C), tailoring their morphology from coarse plate-like or network structures to finer granular or short rod-like shapes and reducing their size[58]; ASMF application in GCr15 bearing steel resulted in a significantly refined microstructures, characterized by a reduced secondary dendrite arm spacing and finer eutectic carbides[63]. Furthermore, MHD-ESR techniques contribute positively to metal cleanliness, another key aspect of solidification quality. TSMF enhances the kinetic conditions for inclusion removal within the LMF, resulting in fewer and smaller inclusions[61] (Fig. 22[58]). EMS has been shown to effectively reduce the size of non-metallic inclusions, particularly large Al_2O_3 particles (>10 μm), and homogenize elemental distribution[59]. Similarly, ASMF improves ingot cleanliness by reducing the count of inclusions larger than 5 μm[63]. These microstructural and cleanliness enhancements translate into improved material properties[58].

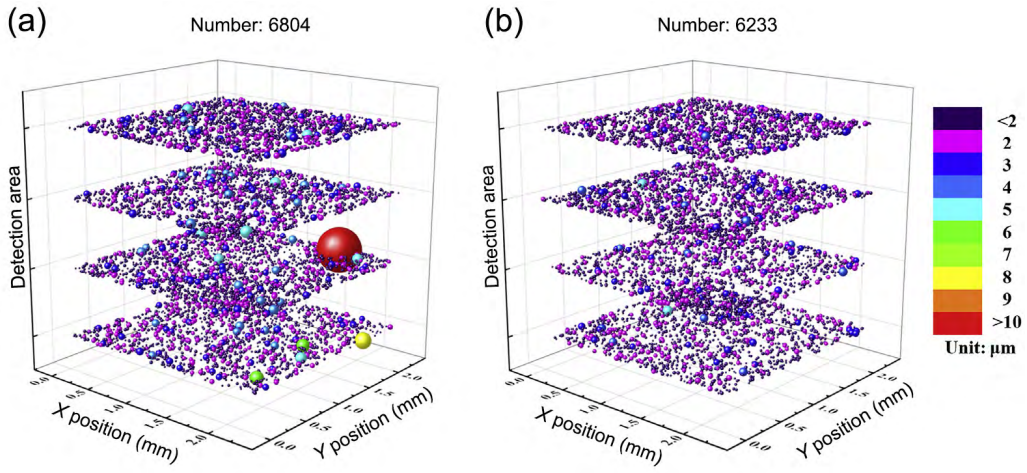

Fig. 22: Number, size, and distribution of inclusions in ESR ingot: (a) 600 A without TSMF; (b) 600 A with TSMF[58]

It is crucial to note that the efficacy of MHD assistance is highly dependent on specific parameters, including the type of field, magnetic flux density (MFD), and, potentially, the current frequency. Optimal MFDs have been identified in several studies (e.g., 65 mT TSMF for M2 steel structure/properties[58], 40 mT ASMF for GCr15 cleanliness/microstructure[63], specific EMS levels for GCr15 cleanliness[59]), beyond which the beneficial effects may plateau or even diminish.

The collective experimental and simulation results firmly establish MHD-ESR as a potent method for controlling the solidification process electromagnetically, leading to refined microstructures, enhanced cleanliness, and improved properties in the final products. However, the integration of magnetic field generation systems increases equipment investment and operational complexity. The optimization of key parameters such as magnetic field strength, frequency, and position is very complex, and the mechanisms of its effect on different material systems require more in-depth research.

4 Control of process atmosphere and pressure in ESR

Complementing the modifications to electrode systems and solidification control strategies, precise management of the process environment, particularly the composition and pressure of the atmosphere surrounding the molten slag and metal, represents another critical aspect of advanced ESR technologies. Control over the gas phase enables targeted manipulation of gas-slag-metal interactions, which exerts a profound influence on chemical reactions, element transfer, gas solubility, and ultimately, the purity and final composition of the remelted material. This section explores three primary approaches for environmental control: (1) the widely adopted practice of conducting ESR under controlled protective gas atmospheres (typically inert Ar or sometimes N_2) at near-atmospheric pressures primarily to prevent ambient contamination (Section 4.1); (2) the application of significantly elevated gas pressures (pressurized ESR, P-ESR, often using N_2) to leverage thermodynamic principles for enhancing gas solubility and suppressing gas-related defects during solidification, particularly in high nitrogen steel production (Section 4.2); and (3) the operation under reduced pressures or vacuum conditions (vacuum ESR, V-ESR) to exploit the low-pressure environment for intensive degassing and promoting specific refining mechanisms like carbon deoxidation (Section 4.3). These atmospheric control measures are employed to minimize or prevent undesirable oxidation, nitridation, and hydrogen pickup from the environment; to facilitate specific refining pathways; to enable the production of alloys with intentionally high dissolved gas contents; to mitigate the loss of volatile or reactive alloying elements; and ultimately, to achieve rigorous control over final chemical composition, residual gas levels (O, N, H), and overall material cleanliness. This addresses limitations commonly encountered in conventional open-air remelting and overcomes challenges that can not be solely resolved through slag chemistry adjustments.

4.1 Gas protective atmosphere ESR

Conducting ESR under a controlled gas protective atmosphere (typically using inert gases) primarily aims to mitigate atmospheric contamination and ensure precise control over the chemical composition and purity of the remelted product[65, 66]. The ingress of oxygen and nitrogen from ambient air during open ESR is a significant source of reoxidation, which leads to the undesirable loss of reactive alloying elements (e.g., Al, Ti, and Si) and an increase in the total oxygen content (T[O]) and nitrogen content ([N]) of the final ingot[65, 67-69]. Implementing a protective atmosphere (exemplified by the schematic principle shown in Fig. 23[70]) effectively shields the molten slag and metal surfaces from direct contact with air, thereby significantly reducing or preventing such reoxidation[66].

Experimental studies comparing protected ESR (under Ar) with conventional ESR for bearing steels (e.g., G20CrNi2Mo) have demonstrated significant reductions in both T[O] and [N], as well as the effective prevention of Al and Ti loss[68]. Similarly, the use of a protective atmosphere (N_2 in the specific study) during ESR of a tool steel significantly reduced Si loss compared to open-air remelting[69]. Beyond controlling the loss of metallic elements and the bulk gas content, protective atmospheres play a crucial role in mitigating hydrogen pickup (Fig. 24[68]), a phenomenon primarily caused by atmospheric moisture interacting with the slag[66, 71]. The impact of protective atmospheres on the cleanliness of non-metallic inclusions is also significant. By preventing reoxidation, protected ESR generally leads to improved cleanliness, characterized by a reduction in the quantity and size of oxide inclusions compared to open ESR, as observed for G20CrNi2Mo bearing steel under Ar[68]. Furthermore, the stable, low-oxygen potential environment maintained by the protective atmosphere enables precise control over deoxidation and inclusion modification treatments (e.g., calcium treatment for modifying $MgO{\cdot}Al_2O_3$ spinels in die steels) unaffected by atmospheric oxygen[72]. Indirectly, by minimizing metal oxidation and maintaining lower levels of oxides like FeO in the slag, protective atmospheres also help sustain optimal slag properties (e.g., high basicity) conducive to other refining reactions such as desulfurization[70-71].

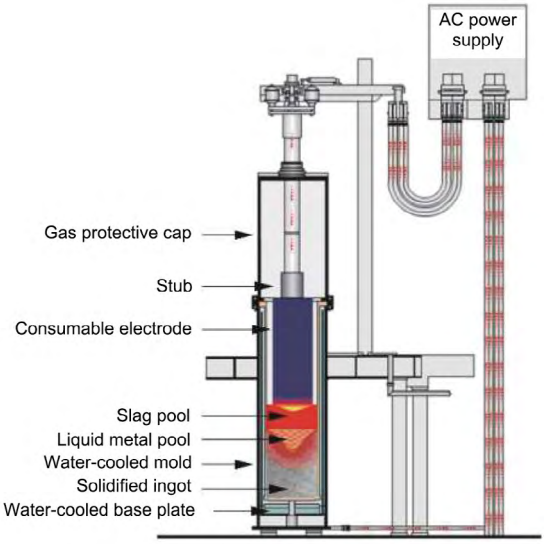

Fig. 23: Schematic diagram of gaseous protection ESR[70]

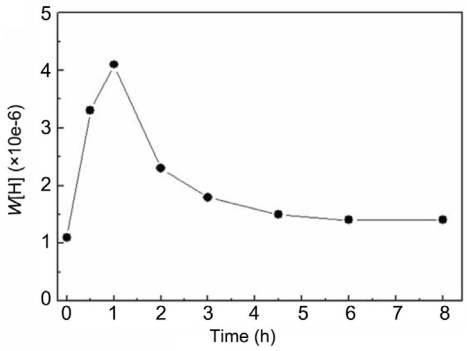

Fig. 24: Curve of hydrogen content in the metallic bath under the dry Ar gas[68]

In substantive terms, controlled protective gas ESR is essential for high-quality steels/alloys requiring precise composition, low gas content, and high cleanliness. While gas protective atmosphere ESR is effective in preventing the oxidation and nitridation of reactive elements, its industrial application faces the following main challenges: (1) Gas atmosphere control: accurately controlling the purity and flow rate of protective gases (e.g., Ar, He, or gas mixtures) in large-scale ESR furnaces to ensure a uniform and stable atmosphere across the entire molten pool and solidification front poses significant technical challenges. Any local gas leakage or introduction of impurities can lead to a decline in casting quality; (2) Cooling effect: some protective gases (e.g., He) exhibit high thermal conductivity, which may remove heat from the molten pool and affect the control of the solidification process.

4.2 Pressurized ESR technology (P-ESR)

P-ESR involves conducting the electroslag process under an elevated pressure controlled gas atmosphere, typically N_2 or inert gas, and represents a crucial technology particularly for the production of high-quality specialty alloys such as high nitrogen steels (HNS)[73-76] (Fig. 25[77]). The primary motivation for employing elevated pressure, especially high N_2 partial pressure, is to significantly increase the solubility of nitrogen in the liquid metal in accordance with Sieverts' law. This, in turn, effectively suppresses the formation of nitrogen porosity during solidification and enables the production of steels with substantially higher nitrogen contents than achievable under atmospheric conditions[74, 78].

Studies investigating the nitrogen transfer mechanism during P-ESR suggest that the predominant pathway for nitrogen pickup is direct transfer from the pressurized gas phase to the exposed liquid metal pool surface, rather than significant dissolution and transfer through the molten slag. Consequently, the nitrogen content in the ingot increases with higher N_2 partial pressure but decreases with greater electrode immersion depth, which reduces the exposed melt surface area (Fig. 26)[79]. Beyond controlling gas solubility and preventing gas-related defects, elevated pressure exerts fundamental influences on

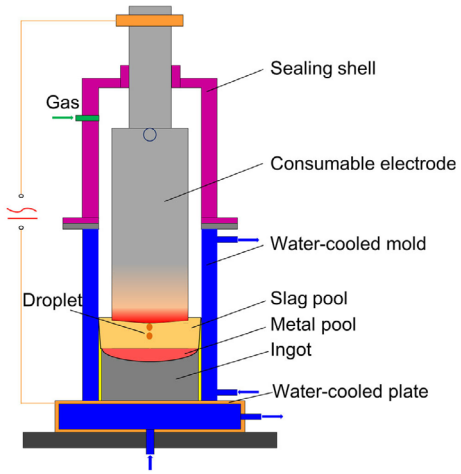

Fig. 25: Schematic diagram of P-ESR furnace[77]

solidification physics. Thermodynamic calculations predict that increased pressure raises the liquidus and solidus temperatures of HNS (e.g., by 6–7 K at 100 MPa for a 22Cr-21Ni-7.5Mo-0.6N steel), potentially alters phase transformation sequences (e.g., suppressing ferrite formation), increases the solidification driving force, reduces the critical nucleation radius, and enhances the nucleation rate, and thereby collectively refines the solidification structure[73, 80]. Furthermore, pressure significantly enhances the interfacial heat transfer coefficient (IHTC) between the solidifying ingot and the mold (e.g., IHTC proportional to $P^{0.21}$ for a cylindrical HNS ingot, where P is pressure, MPa), leading to faster cooling rates[78]. Elevated pressure also modifies the forces acting on non-metallic inclusions during solidification, notably increasing the drag force while having minimal effect on

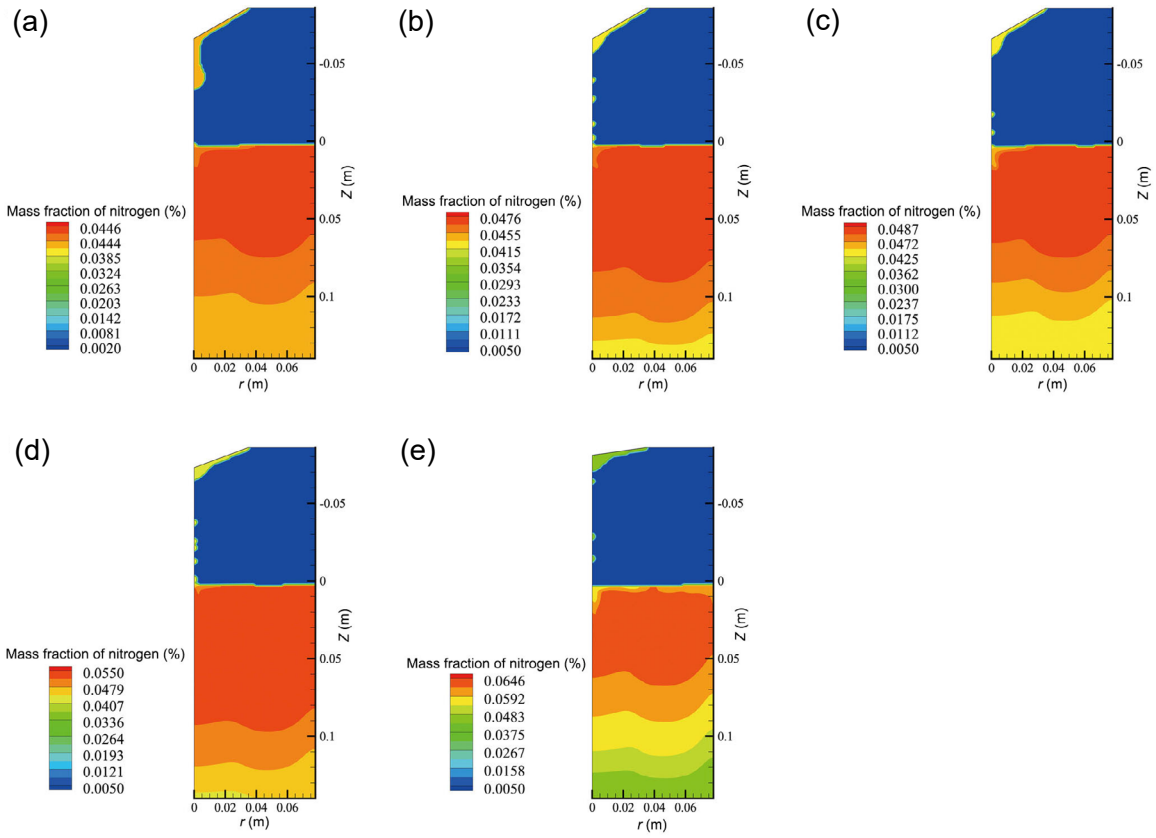

Fig. 26: Nitrogen content in the ingot at t = 1,200 s under various conditions (pressure and electrode depth): (a) 0.1 MPa-20 mm; (b) 0.8 MPa-20 mm; (c) 1.2 MPa-20 mm; (d) 1.2 MPa-13 mm; and (e) 1.2 MPa-5 mm[79], where r is the radius and Z is the height of the ingot

gravity, buoyancy, or thermophoretic forces, thereby altering the movement and final distribution of inclusions within the ingot[80]. However, the pressurized environment exerts a distinct influence on refining reactions compared to open-air or inert gas processes. Specifically, desulfurization during P-ESR under N_2 atmosphere is found to be less effective than that ESR in air, primarily due to the lack of sulfur removal via gasification-oxidation reactions (e.g., SO_2 formation). The pressure level itself shows little direct effect on the slag-metal sulfur distribution, thus necessitating the use of modified slag systems with enhanced sulfur capacity (e.g., Na_2O-containing slags) to achieve adequate desulfurization under pressure[77]. Controlling deoxidation also remains a critical aspect, particularly when processing reactive metals (e.g., titanium alloys) under P-ESR conditions[81].

Nonetheless, P-ESR technology has proven successful in manufacturing various high-performance materials[74, 76], which exhibit desirable properties like enhanced corrosion resistance[75], making them suitable for demanding applications (e.g., high-quality plastic die steels)[76]. The application of pressure is also considered potentially beneficial for increasing the solubility of other volatile elements like Ca or Mg during

specialized refining processes[73].

In summary, P-ESR primarily leverages elevated pressure to control gas solubility for HNS production and fundamentally influences heat transfer, solidification kinetics, and inclusion behavior. It represents a vital tool in advanced metallurgy, although requiring careful management of specific refining reactions (e.g., desulfurization). However, the industrial application of P-ESR faces significant bottlenecks: (1) Equipment design and safety: The high-pressure environment imposes extremely high requirements on the design of the ESR furnace body, requiring high-strength materials and complex sealing structures. This increases both manufacturing costs and potential safety risks, making the furnace's pressure relief and safety control system a key technical challenge; (2) Complexity of process parameters: the coupling of multiple parameters (e.g., pressure, current, voltage, and slag system) makes the optimization of process parameters more complex. How to accurately control the molten pool temperature, solidification rate, and melting rate under high-pressure conditions to achieve the best metallurgical effect is a challenge; (3) Maintenance and operational difficulty: compared to conventional ESR, the maintenance and operation of P-ESR equipment are more complex, requiring operators to possess a higher level of technical proficiency.

4.3 Vacuum ESR technology (V-ESR)

V-ESR represents a specialized refining technique wherein the ESR process is conducted under significantly reduced ambient pressure (i.e., vacuum conditions) as compared to atmospheric pressure or inert gas protected operations. The primary motivation for employing vacuum is to achieve superior levels of material cleanliness, particularly targeting ultra-low oxygen content, and to potentially enhance the solidification microstructure[82, 83]. The schematic diagram of the principle of V-ESR is shown in Fig. 27[83].

A key mechanism underlying the enhanced deoxidation capacity under vacuum is the promotion of carbon deoxidation

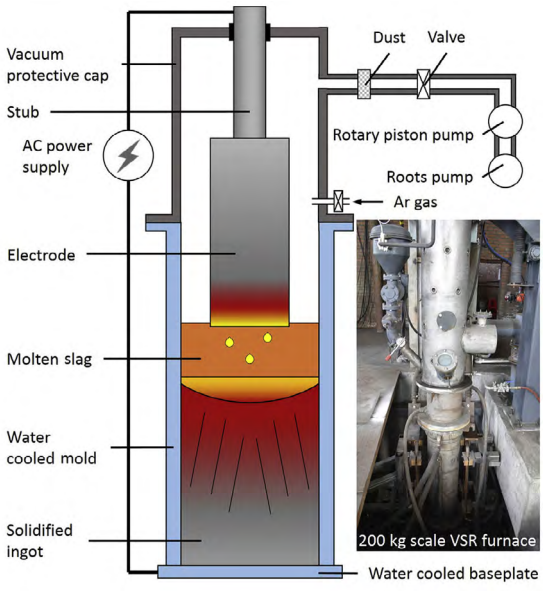

Fig. 27: Schematic diagram of V-ESR furnace[83]

reactions. Thermodynamic calculations and numerical simulations incorporating reaction kinetics indicate that the reduced pressure environment significantly lowers the partial pressure of gaseous reaction products (e.g., carbon monoxide [CO]), thereby thermodynamically favoring the reduction of stable oxides (e.g., Al_2O_3) by dissolved carbon in the steel (e.g., $2[C]+Al_2O_3(s)=2CO(g)+4[Al]$)[84]. Modeling results indicate that carbon deoxidation primarily occurs at the droplet-slag interface and becomes more effective as the vacuum level increases (i.e., lower operating pressure)[83, 84]. Consequently, comparative experimental studies and simulations consistently show that V-ESR results in a lower final T[O] in the remelted ingot compared to ESR performed under Ar protection at atmospheric pressure. For instance, the oxygen content was reported to increase from an initial 13 ppm to 18 ppm under vacuum (10 kPa), versus 24 ppm under Ar (101 kPa)[83], with further predicted reductions at even lower pressures (e.g., down to 14.3 ppm at 1 kPa) (Fig. 28)[84]. This enhanced deoxidation under vacuum directly translates to improved cleanliness, characterized by a lower number density and smaller size of oxide inclusions, particularly Al_2O_3-based ones, compared with conventional or Ar-protected ESR[85] (Fig. 29[82]). Although complex inclusions with multi-layer structures might still be observed, the overall oxide content is reduced under vacuum conditions[86, 87]. Furthermore, V-ESR exerts a significant influence on the solidification structure. Ingots produced via vacuum processing exhibit refined microstructures characterized by smaller secondary dendrite arm spacing (SDAS) and finer pearlite. This refinement is potentially attributable to the faster solidification rate achieved under vacuum conditions[88, 89].

Therefore, V-ESR stands as a critical advanced manufacturing process, leveraging the low-pressure environment to promote carbon deoxidation, minimize residual gas content, reduce oxide inclusions, and refine the solidification microstructure, ultimately yielding materials with exceptional cleanliness and potentially enhanced properties suitable for demanding applications. While V-ESR offers unique advantages in removing volatile impurities, it also presents the following challenges: (1) Slag volatilization: the high-vacuum environment can promote the volatilization of certain components in the molten slag (e.g., CaF_2), alter the slag's composition and properties, and thereby impairing its refining effect. Thus, the design and selection of a suitable low-volatility slag system is a key research focus for V-ESR; (2) High equipment cost and complexity: achieving and maintaining a high vacuum requires a complex vacuum pump system and high-strength vacuum-sealed configurations, which significantly increase the manufacturing and operating costs of the equipment; (3) Process control: under high-vacuum conditions, arc stability can be affected, requiring more precise power supplies and control systems to maintain it. Furthermore, how to balance the effects of vacuum on removing harmful elements and on slag volatilization, and find the optimal process window, is key to its application.

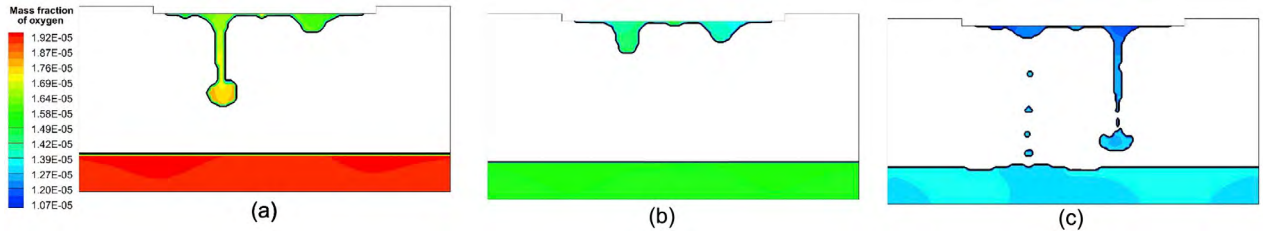

Fig. 28: Predicted distribution of oxygen content in steel under different atmosphere: (a) 101.325 kPa; (b) 10 kPa; and (c) 1 kPa[84]

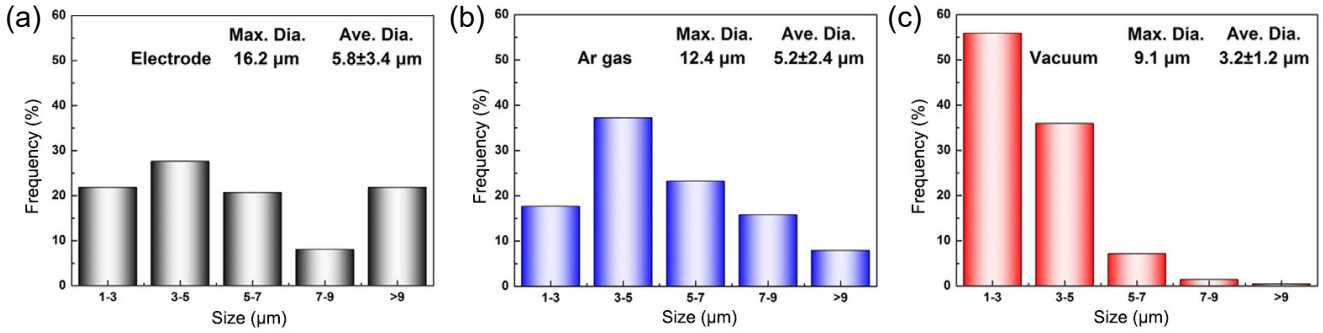

Fig. 29: Size distribution of inclusions observed in the consumable electrode (a), Ar-ESR ingot (b), and vacuum-ESR ingot (c)[82]

5 Summary and outlook

Advanced ESR technologies have significantly expanded the performance boundaries beyond conventional methods, effectively overcoming inherent limitations related to production scale, component complexity, process efficiency, and material purity. The innovations reviewed herein, including dynamic electrode systems, specialized mold designs and operational modes, precise environmental control strategies, and the application of external fields, collectively provide sophisticated means for active control over the entire process from melting to solidification. These developments enable superior metallurgical quality, refined microstructures, enhanced cleanliness, and facilitate the manufacturing of large-sized forgings, intricate near-net shapes, hollow structures, and composite components previously considered challenging or unattainable via conventional ESR practices.

Despite these significant advancements, persistent challenges hinder the broader industrial optimization and widespread adoption of many advanced electroslag techniques. Technical difficulties include ensuring robust process stability and achieving precise, reproducible control, particularly when integrating multiple complex subsystems or operating at very large production scales. The accurate modeling of coupled multiphysics phenomena, essential for understanding and optimization, remains computationally demanding and requires further refinement, particularly with regard to high-temperature slag properties and interfacial behavior. Furthermore, practical barriers, such as the high capital investment for specialized equipment and the lack of widely accepted standards comparable to those for conventional ESR, continue to influence industrial implementation decisions.

Future research and development are poised to further enhance the potential of electroslag technologies. Promising directions include the synergistic integration of multiple advanced methods and the development of intelligent control systems incorporating advanced sensors and artificial intelligence for real-time optimization. Exploring novel manufacturing paradigms, such as ESR casting-welding, which combines casting and welding principles inspired by additive manufacturing concepts to enable the fabrication of ultra-large structures, represents a key growth, and future research should focuses primarily on the fusion zone. Expanding the application scope to new material systems, such as high-entropy alloys or metal matrix composites, potentially via liquid metal processing or in-situ synthesis, alongside the development of hybrid process pathways that combined ESR with other processes (e.g., additive manufacturing or forging), and a sustained emphasis on improving energy efficiency and environmental sustainability, will be crucial to the continued evolution of the technology.

Acknowledgment

This work was supported by the National Natural Science Foundation of China (NSFC 52175352).

Conflict of interest

Prof. Yan-chun Lou is an EBM of *CHINA FOUNDRY*. He was not involved in the peer-review or handling of the manuscript. The authors have no other competing interests to disclose.

References

[1] Ashby M F, Cebon D. Materials selection in mechanical design. Mrs Bulletin, 2005, 30(12): 995.

[2] Marini D, Cunningham D, Corney J R. Near net shape manufacturing of metal: A review of approaches and their evolutions. Proceedings of the Institution of Mechanical Engineers, Part B: Journal of Engineering Manufacture, 2018, 232(4): 650–669.
[3] Jawahir I S, Attia H, Biermann D, et al. Cryogenic manufacturing processes. CIRP Annals – Manufacturing Technnology, 2016, 65(2): 713–736.
[4] Medovar L, Stovpchenko G, Sybir A, et al. Electroslag hollow ingots for nuclear and petrochemical pressure vessels and pipes. Metals, 2023, 13(7): 1290.
[5] Medovar B I and Boyko G A (Eds). Electroslag technology. Springer Science & Business Media, 2013.
[6] Arh B, Podgornik B, Burja J. Electroslag remelting: A process overview. Materiali in Tehnologije, 2016, 50(6): 971–979.
[7] Li Z B. Principle and application of electroslag metallurgy. Beijing: Metallurgical Industry Press, 1996: 104–120. (In Chinese)
[8] Kharicha A, Karimi-Sibaki E, Wu M H, et al. Review on modeling and simulation of electroslag remelting. Steel Research International, 2018, 89(1): 1700100.
[9] Dub V S, Levkov L Y, Shurygin D A, et al. Electroslag remelting technology for contemporary engineering, retrospection and new possibilities. Metallurgist, 2018, 62(5): 511–520.
[10] Paton B E, Medovar L B. Improving the electroslag remelting of steel and alloys. Steel in Translation, 2008, 38(12): 1028–1032.
[11] Medovar L B, Stovpchenko A P, Saenko V Y, et al. Concept of a universal ESR furnace for the production of large ingots. Russian Metallurgy (Metally), 2011, 2011: 1118–1123.
[12] Xiong Y L, Song Z W, Wang A G, et al. Factors influencing power consumption and power-saving measures in ESR process. China Foundry, 2019, 16(1): 1–7.
[13] Wang A G, Gao Z H, Zhang L, et al. Review on technology progress of electroslag casting products. International Journal of Metalcasting, 2025, 19: 3056–3071.
[14] Wang F, Lou Y C, Chen R, et al. Effect of vibrating electrode on temperature profiles, fluid flow, and pool shape in ESR system based on a comprehensive coupled model. China Foundry, 2015, 12(4): 285–292.
[15] Wang F, Wang Q, Lou Y C, et al. Investigation of heat transfer and magnetohydrodynamic flow in electroslag remelting furnace using vibrating electrode. JOM, 2016, 68: 410–420.
[16] Zhang C M. Research on melting rate and solidification organization of vibrating electrode method in ESR process. Master's Dissertation, Academy of Machinery Science and Technology Group Co., Ltd., 2015. (In Chinese)
[17] Wang F, Wang Q, Li B K. Comparison of thermo-electromagneto-hydrodynamic multi-physical fields in ESR furnace with vibrating and traditional electrodes. ISIJ International, 2017, 57(1): 91–99.
[18] Song Z W, Chen R, Xiong Y L, et al. Effect of electrode vibration on inclusions of ZG04Cr13Ni4Mo stainless steel during electroslag casting. Foundry, 2015, 64(11): 1108–1112. (In Chinese)
[19] Chumanov I V, Chumanov V I. Technology for electroslag remelting with rotation of the consumable electrode. Metallurgist, 2001, 45(3): 125–128.
[20] Chumanov I V, Matveeva M A, Sergeev D V. Influence of electrode rotation in electroslag remelting on the anisotropy of ingot properties. Steel in Translation, 2019, 49: 77–81.
[21] Huang X C, Li B K, Liu Z Q, et al. Modeling of fluid flow, heat transfer and inclusion removal in electroslag remelting process with a rotating electrode. International Journal of Heat and Mass Transfer, 2020, 163: 120473.
[22] Chumanov I V, Anikeev A N. Calculation of the end form the rotating electrode in the liquid environment. IOP Conference Series: Materials Science and Engineering, 2017, 241: 012017.
[23] Wang Q, Gosselin L, Li B K. Effect of rotating electrode on magnetohydrodynamic flow and heat transfer in electroslag remelting process. ISIJ International, 2014, 54(12): 2821–2830.
[24] Huang X C, Liu Z Q, Li B K, et al. A three-dimensional multiphysics coupled model of melting and rotation of the electrode during electroslag remelting process. Metallurgical and Materials Transactions: B, 2024, 55(2): 667–681.
[25] Huang X C, Duan Y R, Liu Z Q, et al. Role of electrode rotation on improvement of metal pool profile in electroslag remelting process. Metals, 2021, 11(11): 1675.
[26] Anikeev A N, Chumanov I V, Sergeev D V. Effect of rotating electrode technology on the corrosion resistance of a low-carbon chromium containing steel. AIP Conference Proceedings, 2017, 1886: 020064.
[27] Liu Z L, Medovar L, Stovpchenko G, et al. Phenomena at three-phase electroslag remelting. China Foundry, 2021, 18(6): 557–564.
[28] Li B K, Wang B W, Tsukihashi F. Modeling of electromagnetic field and liquid metal pool shape in an electroslag remelting process with two series-connected electrodes. Metallurgical and Materials Transactions: B, 2014, 45: 1122–1132.
[29] Wang F, Wang Q, Baleta J, et al. Sequentially coupled simulation of multiphysical fields during twin-electrode electroslag remelting process. Metallurgical and Materials Transactions: B, 2020, 51: 2285–2297.
[30] Wang Q, Qi F S, Wang F, et al. Numerical investigation on electromagnetism and heat transfer in electroslag remelting process with triple-electrode. International Journal of Precision Engineering and Manufacturing, 2015, 16: 2467–2474.
[31] Ren N, Li B K, Li L M, et al. Numerical investigation on the fluid flow and heat transfer in electroslag remelting furnace with triple-electrode. Ironmaking & Steelmaking, 2018, 45(2): 125–134.
[32] Zang X M, Qiu T Y, Li W M, et al. Electroslag remelting withdrawing technology for offshore jack-up platform rack steel manufacturing process. Journal of Iron and Steel Research, International, 2016, 23(4): 297–304.
[33] Li W M, Jiang Z H, Zang X M, et al. Modeling of flow and temperature distribution in electroslag remelting withdrawal process for fabricating large-scale slab ingots. Journal of Iron and Steel Research, International, 2017, 24(6): 569–578.
[34] Liu F B, Jiang Z H, Li H B, et al. Mathematical modelling of electroslag remelting P91 hollow ingots process with multi-electrodes. Ironmaking & Steelmaking, 2014, 41(10): 791–800.
[35] Wang A G, Jiang Z H, Lou Y C, et al. Up-pulling force analysis for ESC hollow cylindrical casting. China Foundry, 2020, 17(1): 48–55.
[36] Yang M. Numerical simulation of ESC by fixed consumable electrode filling method. Doctoral Dissertation, Anshan Liaoning: Liaoning University of Technology, 2017. (In Chinese)
[37] Wang J, Chang G W, Chen R. Electroslag casting by fixed consumable electrode filling method. Foundry Technology, 2020, 41(9): 881–886. (In Chinese)
[38] Zhao L T, Chen R, Xiong Y L. Study on liquid metal supplement speed of electroslag casting with the filling method of fixed consumable electrode. Foundry, 2018, 67(9): 767–771. (In Chinese)
[39] Zhao L T, Xiong Y L, Chen R, et al. Correlation between current and cross-sectional area of parallel fixed-movable dual electrodes in ESC. China Foundry, 2020, 17(3): 245–249.

[40] Zhao L T, Li B D, Xiong Y L, et al. Study on dynamic characteristics of the filling method of fixed consumable electrode. Foundry, 2017, 66(7): 727–730. (In Chinese)
[41] Yang M, Chang G W, Chen R. Study on bottom formability of ESC ingots by filling method of fixed consumable electrode. Journal of Iron and Steel Research, 2018, 30(12): 970–976. (In Chinese)
[42] Li X, Jiang Z H, Geng X, et al. Numerical simulation of a new electroslag remelting technology with current conductive stationary mold. Applied Thermal Engineering, 2019, 147: 736–746.
[43] Dong Y W, Jiang Z H, Cao H, et al. Study of single-power, two-circuit ESR process with current-carrying mold: Development of the technique and its physical simulation. Metallurgical and Materials Transactions: B, 2016, 47: 3575–3581.
[44] Dong Y W, Jiang Z H, Cao H B, et al. A novel single power two circuits electroslag remelting with current carrying mould. ISIJ International, 2016, 56(8): 1386–1393.
[45] Liu F B, Zang X M, Jiang Z H, et al. Removal of non-metallic inclusions in current-conductive mold ESR process. China Metallurgy, 2010, 20(5): 5–8. (In Chinese)
[46] Hou D, Liu F B, Qu T P, et al. Behavior of alloying elements during drawing-ingot-type electroslag remelting of stainless steel containing titanium. ISIJ International, 2018, 58(5): 876–885.
[47] Alghisi D, Milano M, Pazienza L. From ESR to continuous CC-ESRR process: Development in remelting technology towards better products and productivity. La Metallurgia Italiana, 2005, 1: 21–32.
[48] Lu P, Ye M Z. Process technology and equipment of withdrawal electroslag remelting furnace. Modern Metallurgy, 2010, 38(3): 17–19. (In Chinese)
[49] Qi H Y, Li X C, Li W M, et al. Distribution law of flow field and temperature field in electroslag remelting withdrawal process. Journal of Iron and Steel Research, 2018, 30(4): 294–301. (In Chinese)
[50] Karimi-Sibaki E, Kharicha A, Wu M, et al. A multiphysics model of the electroslag rapid remelting (ESRR) process. Applied Thermal Engineering, 2018, 130: 1062–1069.
[51] Guo H L, Guo L P. Discussion about reason of steel leakage in slab electroslag furnace with stripping-type mold. Hebei Metallurgy, 2012, 11: 36–38. (In Chinese)
[52] Chang L Z, Shi X F, Cong J Q, et al. Effects of relative motion between consumable electrodes and mould on solidification structure of electroslag ingots during electroslag remelting process. Ironmaking & Steelmaking, 2014, 41(8): 611–617.
[53] Shi X F, Chang L Z, Wang J J. Effect of mold rotation on the bifilar electroslag remelting process. International Journal of Minerals, Metallurgy, and Materials, 2015, 22: 1033–1042.
[54] Deng N Y, Shi X F, Chen J S, et al. Numerical simulation of mold rotation and its effect on carbides in HSS ESR ingot. Chinese Journal of Engineering, 2020, 42(4): 516–526. (In Chinese)
[55] Chang L Z, Chang K H, Zhu X M, et al. Effect of mold rotation on inclusions in ESR ingot. The Chinese Journal of Process Engineering, 2019, 19(6): 1186–1196. (In Chinese)
[56] Chang L Z, Su Y L, Xu T, et al. A preliminary exploration on improving the solidification quality of electroslag ingot based on laboratory scale experiment. Ironmaking & Steelmaking, 2022, 49(10): 995–1004.
[57] Shi X F, Chang L Z, Wang J J. Effect of ultrasonic power introduced by a mold copper plate on the solidification process. International Journal of Minerals, Metallurgy, and Materials, 2017, 24: 139–146.
[58] Guo Y F, Qi W T, Xia Z B, et al. Morphology tailoring of metal pool and eutectic carbides in magnetic-controlled electroslag remelted M2 high-speed steel. Journal of Materials Research and Technology, 2022, 16: 1122–1135.
[59] Shi X F, Xu T, Chang L Z. Effect of electromagnetic stirring on metallurgical quality of GCr15 electroslag ingot. China Foundry, 2022, 19(1): 46–54.
[60] Guo Y F, Ma C K, Xia Z B, et al. Morphology tailoring and enhanced inclusion removal of liquid melt film by regulating the magnetic flux density during magnetic controlled ESR process. Metallurgical and Materials Transactions: B, 2021, 52: 3383–3392.
[61] Wang H, Zhong Y B, Li Q, et al. Effect of current frequency on droplet evolution during magnetic-field-controlled electroslag remelting process via visualization method. Metallurgical and Materials Transactions: B, 2017, 48: 655–663.
[62] Wang H, Zhong Y B, Li Q, et al. Influences of the transverse static magnetic field on the droplet evolution behaviors during the low frequency electroslag remelting process. ISIJ International, 2017, 57(12): 2157–2164.
[63] Li Q, Xia Z B, Guo Y F, et al. Effect of axial static magnetic field on cleanliness and microstructure in magnetically controlled electroslag remelted bearing steel. Journal of Iron and Steel Research International, 2021, 28: 1562–1573.
[64] Igizianova N A, Sokolova E V. Modeling electromagnetic processes in direct current electroslag remelting. The International Journal of Advanced Manufacturing Technology, 2021, 113: 3189–3193.
[65] Duan S C, Shi X, Wang F, et al. A review of methodology development for controlling loss of alloying elements during the electroslag remelting process. Metallurgical and Materials Transactions: B, 2019, 50: 3055–3071.
[66] Shi C B. Deoxidation of electroslag remelting (ESR) – A review. ISIJ International, 2020, 60(6): 1083–1096.
[67] Chang L Z, Shi X F, Cong J Q. Study on mechanism of oxygen increase and countermeasure to control oxygen content during electroslag remelting process. Ironmaking & Steelmaking, 2014, 41(3): 182–186.
[68] Zhan D P, Zhang Y P, Liu R J, et al. Effect of protected electroslag remelting on cleanliness of G20CrNi2Mo bearing steel. Ironmaking & Steelmaking, 2017, 44(5): 368–376.
[69] Schneider R S E, Molnar M, Gelder S, et al. Effect of the slag composition and a protective atmosphere on chemical reactions and non-metallic inclusions during electro-slag remelting of a hot-work tool steel. Steel Research International, 2018, 89(10): 1800161.
[70] Shi C B, Huang Y, Zhang J X, et al. Review on desulfurization in electroslag remelting. International Journal of Minerals, Metallurgy and Materials, 2021, 28: 18–29.
[71] Yan C, Li Y, Ma B Y, et al. Parameters optimising of the protective gas electroslag remelting. Materials Research Innovations, 2015, 19(sup1): 62–65.
[72] Shi C B, Chen X C, Guo H J, et al. Control of $MgO{\cdot}Al_2O_3$ spinel inclusions during protective gas electroslag remelting of die steel. Metallurgical and Materials Transactions: B, 2013, 44: 378–389.
[73] Zhu H C, Jiang Z H, Li H B, et al. Effect of pressurization technology on steel-making and solidification of high-grade special steels. Iron and Steel, 2015, 50(11): 37–44. (In Chinese)
[74] Li H B, Jiang Z H, Ma Q F, et al. Manufacturing high nitrogen austenitic stainless steels by pressurized induction furnace. Applied Mechanics and Materials, 2011, 52: 1687–1691.
[75] Feng H, Li H B, Jiang Z H, et al. Designing for high corrosion-resistant high nitrogen martensitic stainless steel based on DFT calculation and pressurized metallurgy method. Corrosion Science, 2019, 158: 108081.
[76] Kang C P, Liu F B, Zheng H B, et al. Microstructure evolution and mechanical properties of PESR 55Cr17Mo1VN plastic die steel during quenching and tempering treatment. Journal of Iron and Steel Research International, 2021, 28: 1625–1633.

[77] Yang S X, Li H B, Feng H, et al. Desulfurization behavior of Fe-18Cr-18Mn alloy during the pressurized electroslag remelting with different atmospheres and Na_2O-containing slags. Metallurgical and Materials Transactions: B, 2021, 52: 1294–1308.
[78] Zhu H C, Li H B, Jiang Z H, et al. Quantitative correlation between interfacial heat transfer coefficient and pressure for 19Cr-14Mn-0.9N high nitrogen steel cylindrical ingot. ISIJ International, 2020, 60(9): 1978–1984.
[79] Yu J, Liu F B, Li H B, et al. Numerical simulation and experimental investigation of nitrogen transfer mechanism from gas to liquid steel during pressurized electroslag remelting process. Metallurgical and Materials Transactions: B, 2019, 50: 3112–3124.
[80] Zhu H C, Li H B, He Z Y, et al. Effect of pressure on inclusion number distribution during the solidification process of H13 die steel ingot. Metallurgical and Materials Transactions: B, 2020, 51: 2976–2992.
[81] Bartosinski M, Hassan-Pour S, Friedrich B, et al. Deoxidation limits of titanium alloys during pressure electro slag remelting. IOP Conference Series: Materials Science and Engineering, 2016, 143: 012009.
[82] Liu Y, Wang X J, Li G Q, et al. Cleanliness improvement and microstructure refinement of ingot processed by vacuum electroslag remelting. Journal of Materials Research and Technology, 2020, 9(2): 1619–1630.
[83] Huang X C, Li B K, Liu Z Q, et al. Oxygen transport behavior and characteristics of nonmetallic inclusions during vacuum electroslag remelting. Vacuum, 2019, 164: 114–120.
[84] Huang X C, Li B K, Liu Z Q, et al. Numerical study on the effect of vacuum on oxygen transfer in electroslag remelting process. Vacuum, 2020, 172: 109069.
[85] Huang X C. Study on the heat and mass transfer and inclusion behavior during the production of clean steel using electroslag remelting process. Doctroal Dissertation, Shenyang China: Northeastern University, 2021. (In Chinese)
[86] Liu Y, Zhang Z, Li G Q, et al. Evolution of desulfurization and characterization of inclusions in dual alloy ingot processed by electroslag remelting. Steel Research International, 2017, 88(11): 1700058.
[87] Liu Y. Fundamental research on preparation of ultra clean dual alloy ingot by vacuum electroslag remelting. Doctroal Dissertation, Wuhan China: Wuhan University of Science and Technology, 2019. (In Chinese)
[88] Liu Y, Zhang Z, Li G Q, et al. The structural evolution and segregation in a dual alloy ingot processed by electroslag remelting. Metals, 2016, 6(12): 325.
[89] Liu Y, Zhang Z, Li G Q, et al. Effect of current on structure and macrosegregation in dual alloy ingot processed by electroslag remelting. Metals, 2017, 7(6): 185.